

Hall-Petch Relationship in an Al-Mg-Sc Alloy Subjected to ECAP

A. Dubyna^{1,a}, A. Mogucheva^{1,b}, R. Kaibyshev^{1,c}

¹Belgorod State University, Pobeda 85, Belgorod 308015, Russia

^adubyna@bsu.edu.ru, ^bmogucheva@bsu.edu.ru, ^crustam_kaibyshev@bsu.edu.ru

Keywords: aluminum alloys, equal channel angular pressing, mechanical properties, ultrafine grained microstructure

Abstract. Effect of extensive grain refinement on mechanical properties of an Al-Mg-Sc alloy subjected to equal-channel angular pressing (ECAP) at 300°C is considered in detail. It was shown that the Hall-Petch relationship with the coefficient, k_y , of $0.2 \text{ MPa}\times\text{m}^{1/2}$ is valid in a wide strain range despite a great difference in deformation structures. Volume fraction of fine grains with an average size of $\sim 1 \mu\text{m}$ gradually increases with strain. It is caused by the fact that additive contributions of grain size strengthening and dislocation strengthening to the overall strengthening take place in this alloy. Upon ECAP the extensive grain refinement is accompanied by increasing dislocation density. Superposition of deformation and structural strengthening mechanisms provides achieving very high strength in the alloy. It was shown that ECAP at 300°C has no remarkable effect on a dispersion of coherent dispersoids, $\text{Al}_3(\text{Sc,Zr})$, which gives a significant contribution to overall strength through dispersion strengthening. Contributions of different strengthening mechanisms to overall strength of the material are analyzed.

Introduction

The Al-Mg alloys (5XXX series) exhibit low-to-moderate yield strength (YS) ranging from 90 to 160 MPa for different Mg content [1]. Micro-alloying additions of Sc may provide upwards of 50% increases in the YS due to the formation of coherent Al_3Sc precipitates with size ranging from 7 to 20 nm [2,3]. The another method of strengthening these materials is work hardening [1,2]. $\text{Al}_3(\text{Sc,Zr})$ dispersoids may significantly enhance work hardening effect in Al-mg alloys [4]. In addition, a significant increase in strength of Al-Mg alloys could be attained through the formation of ultra-fine grained (UFG) structure using equal-channel angular pressing (ECAP) [5-7]. Increased strength in materials with UFG structure is attributed through the grain size strengthening in accordance with the well-known Hall-Petch relationship [5-7]:

$$\sigma_y = \sigma_0 + k_y d^{-1/2} \quad (1)$$

where σ_0 and k_y are constants determined experimentally. In general, the formation of UFG leads to +50% increase in YS in comparison with coarse grained (CG) reference Al-Mg alloys [4-6]. Recently, it was shown [7] that the extensive grain refinement through high pressure torsion (HPT) provided +300% increase in YS up to superior value of 900 MPa in an Al-6%Mg-0.3%Sc alloy. However, interpretation of this hardening only in terms of Hall-Petch strengthening is ambiguous. The 5XXX series alloys exhibit poor Hall-Petch response with k_y value ranging from 0.15 to 0.26 $\text{MPa}\times\sqrt{\text{m}}$ [8,9]. Therefore, even the formation of nanoscale grained structure could not provide such the great increment in the YS value. There are limited number of studies were dealt with examination of the Hall-Petch relationship in Al-Mg alloys. The aim of the present study is to establish the potential of grain refinement through ECAP in achieving high strength with retention of ductility at sufficiently high level in an Al-Mg-Sc alloy.

Material and Experimental Procedures

The experiments were conducted using an aluminium alloy with a chemical composition of Al-6Mg-0.5Mn-0.2Sc-0.07Zr (in wt.%), which was developed in Russia and designated as 1570Al. It is worth noting that the last grade of this alloy, which is distinguished from early version of the

1570Al [7,10] by Zr additions and lower Sc content was examined. The initial material was supplied in form of a bar extruded in the temperature interval 380-340°C with ratio 4:1. This rod was cut into rectangular plates with dimensions of 20×20×100 mm³. Next, these billets were processed through ECAP with a back pressure of 20% ram pressure up to total strains of ~1, ~2, ~4, ~8, ~12 at a temperature of 300°C using route B_C. Other details of ECAP and structural characterization were reported in previous works [10,11].

Tensile specimens with a 25 mm gage length and 3 mm width were machined from the extruded bar and the billets subjected to ECAP with tension axis parallel to the extrusion direction or last ECAP axis. The samples were tensioned to failure at room temperature using an Instron 5882 testing machine.

Experimental results

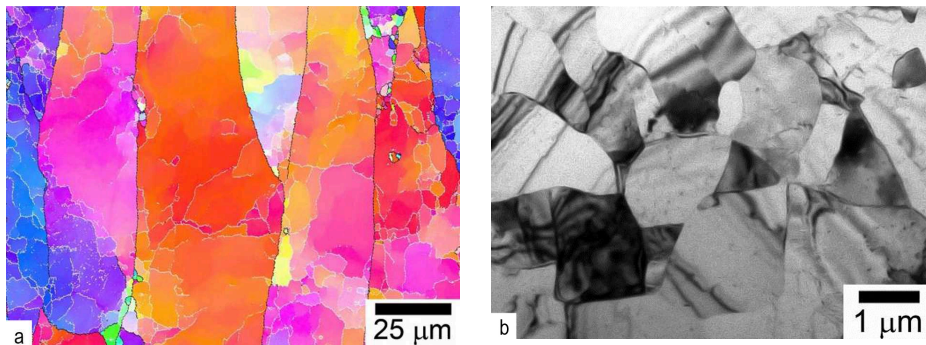


Fig.1. Initial microstructure. Misorientation map (a), TEM micrograph (b).

Initial structure consists of initial grains elongated along the extrusion direction and negligible volume fraction (~0.02) of recrystallized grains with an average size of ~3 μm and round shape (Fig.1a). Average dimensions of coarse grains in the extrusion and transverse directions were ~75 and ~20 μm, respectively.

The fraction of high-angle boundaries (HAB) was ~26%, and the average misorientation was 13°. Low-angle boundaries (LAB) with misorientation of 2° or higher subdivide interiors of elongated grains on subgrains with essentially equiaxed shape and size ranging from 10 to 25 μm (Fig.1a), while well-defined subgrains delimited by LABs with misorientation <2° could be revealed by TEM within interiors of initial grains (Fig.1b). The densities of the lattice dislocations was not so high ($\rho \sim 1.6 \times 10^{13} \text{ m}^{-2}$) (Fig.1b). Two types of nanoscale dispersoids were observed. Coherent Al₃(Sc,Zr) dispersoids having a size of ~10 nm were very uniformly distributed. These particles exhibit well-defined coffee bean contrast indicating high coherent stress. Particles of Al₆Mn phase having incoherent interfaces with round shape and an average size of ~36 nm were rarely observed.

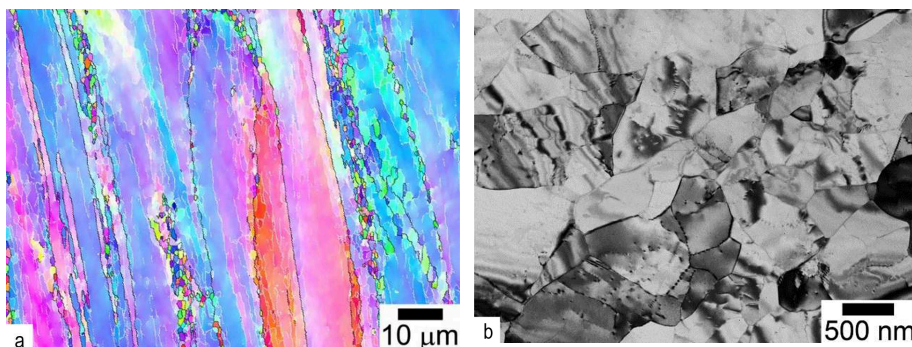


Fig.2. Deformation structure after $\epsilon \sim 1$. (a) misorientation map (b) TEM micrograph.

Deformation structure.

First pass leads to re-orientation of initial boundaries at angle of ~27° to the direction of inlet channel (Fig.2a). In addition, planar geometrically necessary boundaries (GNB) evolve along this direction (Fig.2a). Most of these boundaries have misorientation less than

2° (Fig.2). At $\epsilon \sim 1$, portion of HABs and average misorientation attained 30% and 17°, respectively. Lattice dislocation density increases by a factor of 6 up to $\rho \sim 9 \times 10^{13} \text{ m}^{-2}$. New recrystallized grains with round shape and an average size of ~1.1 μm evolve; their volume fraction attains 7% (Fig.2a).

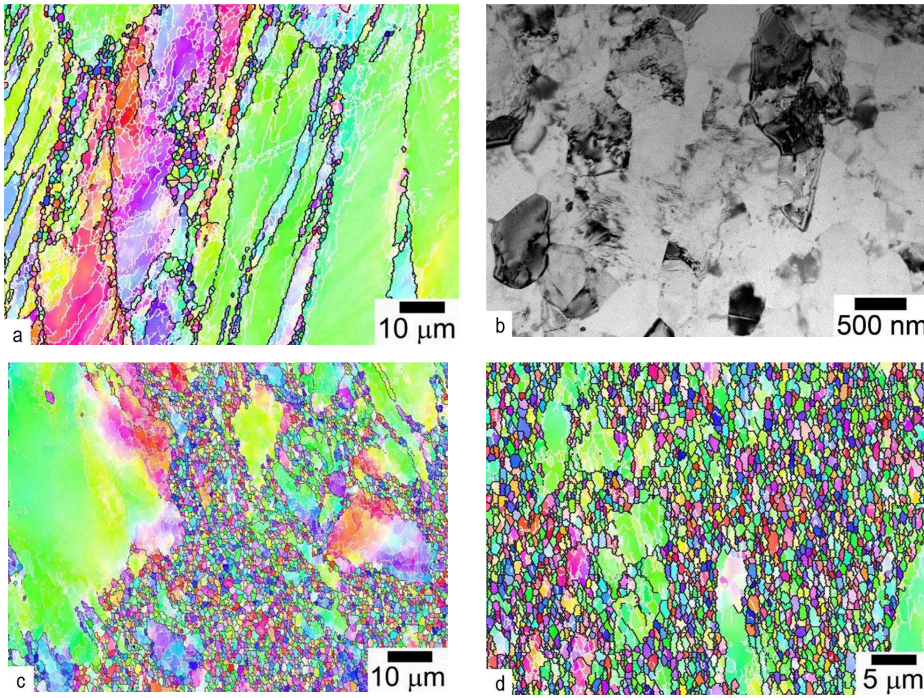


Fig.3. Deformation structure. (a) $\epsilon \sim 2$, misorientation map; (b) $\epsilon \sim 4$, TEM micrograph; (c) $\epsilon \sim 4$, misorientation map; (d) $\epsilon \sim 8$, misorientation map

At $\epsilon \sim 2$, the formation of 2nd order GNBs at an angle of $\sim 120^\circ$ to 1st order GNBs initiates the transformation of lamellar structure to granular one (Fig.3a). Therefore, the formation of 3D arrays of LABs start to occur at $\epsilon > 1$. Average misorientation and portion of HABs remain almost unchanged despite the fact that 1st order GNBs tend to acquire high-angle misorientation. It is attributed to the extensive formation of LABs that overcompensated the transformation of some LABs to HABs. The density of lattice dislocations increases to $\rho \sim 2.1 \times 10^{14} \text{ m}^{-2}$. Volume fraction of recrystallized grains insignificantly increases up to 0.1. For $\epsilon \sim 4$, a partially recrystallized structure evolves. Recrystallized fraction strongly increases and attains 35%. Distinct areas of fully recrystallized grains with an average size of $\sim 1 \mu\text{m}$ alternate with unrecrystallized grains (Fig.3b). Remnants of initial grains are subdivided by LABs with misorientation less than 2° to subgrains exhibiting elongated shape (Fig.3c). The HAB

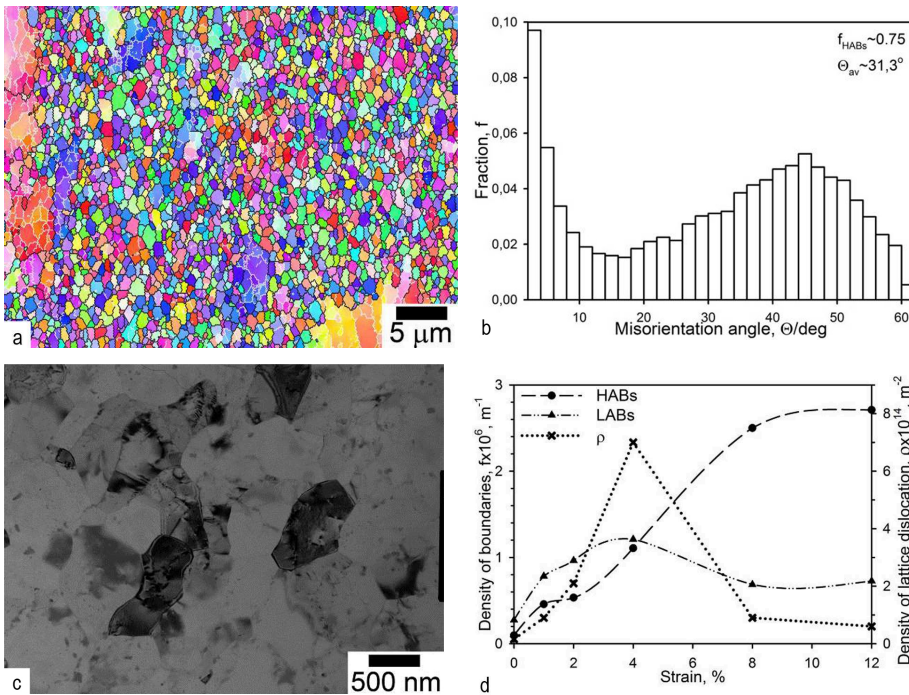


Fig.4. Deformation structure at $\epsilon \sim 12$. (a) misorientation map, (b) misorientation distribution, (c) TEM micrograph (d) effect of strain on densities of HABs, LABs and dislocation density

HABs and LABs takes place in this strain interval (Fig.4d).

fraction and the average misorientation attain $\sim 45\%$ and $\sim 20^\circ$, respectively. It is worth noting that most of crystallite are grains entirely delimited by HABs or subgrains entirely bounded by LABs with low misorientation. Lattice dislocation density attain very high value of $\sim 7 \times 10^{14} \text{ m}^{-2}$. Therefore, up to $\epsilon \sim 4$, volume fraction of recrystallized grains increases concurrently with increasing density of LABs and density of lattice dislocations (Fig.4d). It is worth noting that continuous increase in density of

fraction and the average misorientation attain $\sim 45\%$ and $\sim 20^\circ$, respectively. It is worth noting that most of crystallite are grains entirely delimited by HABs or subgrains entirely bounded by LABs with low misorientation. Lattice dislocation density attain very high value of $\sim 7 \times 10^{14} \text{ m}^{-2}$. Therefore, up to $\epsilon \sim 4$, volume fraction of recrystallized grains increases concurrently with increasing density of LABs and density of lattice dislocations (Fig.4d). It is worth noting that continuous increase in density of

Upon further strain the volume fraction of recrystallized grains, portion of HABs and average misorientation increase continuously and at $\varepsilon \sim 12$, fully recrystallized structure evolves (Fig.4). Volume fraction of unrecrystallized grains is less than 10% (Fig.4a); portion of HABs is 75% and average misorientation is $\sim 32^\circ$ (Fig.4b). It is known [12] that if the fraction of HABs is >0.64 or $0.7-0.75$ an aluminum alloy undergoes continuous dynamic recrystallization (CDRX) and UFG structure evolved. Most of HABs contain low density of grain boundary dislocations (Fig.4c), density of lattice dislocations decreases by a factor of ~ 8 in comparison with at $\varepsilon = 4$ and is $\rho \sim 7 \times 10^{13} \text{ m}^{-2}$. Therefore, at $\varepsilon > 4$, growth of recrystallized fraction is accompanied by drop in density of lattice dislocations (Fig.4d). Decreasing density of LABs and increasing density of HABs (Fig.4d) are attributed to gradual transformation of LABs evolved at $\varepsilon \leq 4$ to HABs. The formation of low number of deformation-induced LABs takes place in this strain interval.

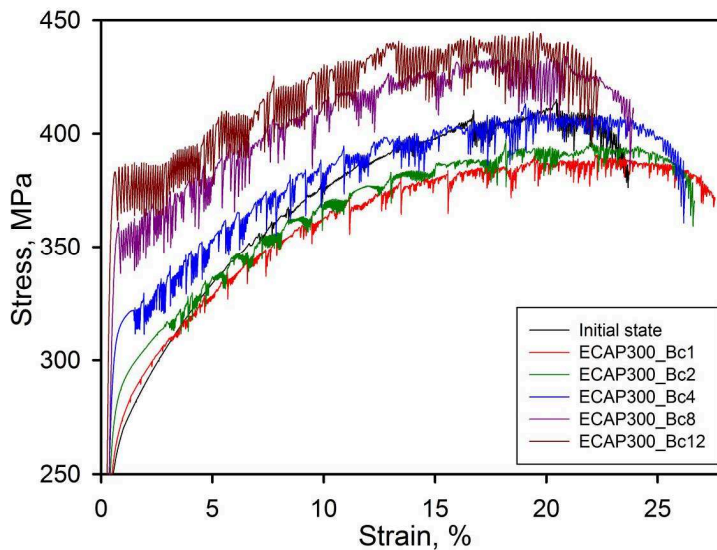


Fig.5 Engineering σ - ε curves aluminium alloy 1570 after ECAP

Mechanical properties. The engineering σ - ε curves are presented in Fig. 5. The serrated flow associated with the Portevin Le Chatelier (PLC) effect is manifested as repeating oscillations on the stress-strain curves (Fig. 5). Increasing strain leads to increase both in amplitude of these oscillations and their frequency. It is apparent that transition from the so-called type A serrations distinguished as an abrupt rise in the stress followed by a drop to or below the general level of flow stress on the σ - ε curve [13] to type B serration, in which oscillations appear with high frequency stress

jumps [13], takes place with increasing strain. Therefore, the formation of recrystallized grains in the 1570Al affects the serration type as increasing temperature [13]. It is known [13] that plastic instability attributed to PLC effects yields low ductilities. However, in the present alloy the strain hardening is high enough to provide elongation-to-failure $>20\%$ after all passes. The change in serration type has a minor effect on ductility, and, therefore, manifestation of PLC effect is insignificantly important for mechanical properties of the 1570Al subjected to ECAP.

The YS, ultimate tensile strengths (UTS) and elongation-to-failure (δ) are summarized in Table I. It is seen increasing strain leads to gradual increase in YS and UTS values; ductility remains nearly unchanged.

Table I Mechanical properties aluminium alloy after ECAP

Processing	YS [MPa]	UTS [MPa]	δ [%]
1570-initial	250	410	22,0
1570-ECAP300_Bc1	255	390	26,5
1570-ECAP300_Bc2	280	395	25,0
1570-ECAP300_Bc4	305	410	24,0
1570-ECAP300_Bc8	355	430	23,0
1570-ECAP300_Bc12	385	445	20,5

Discussion

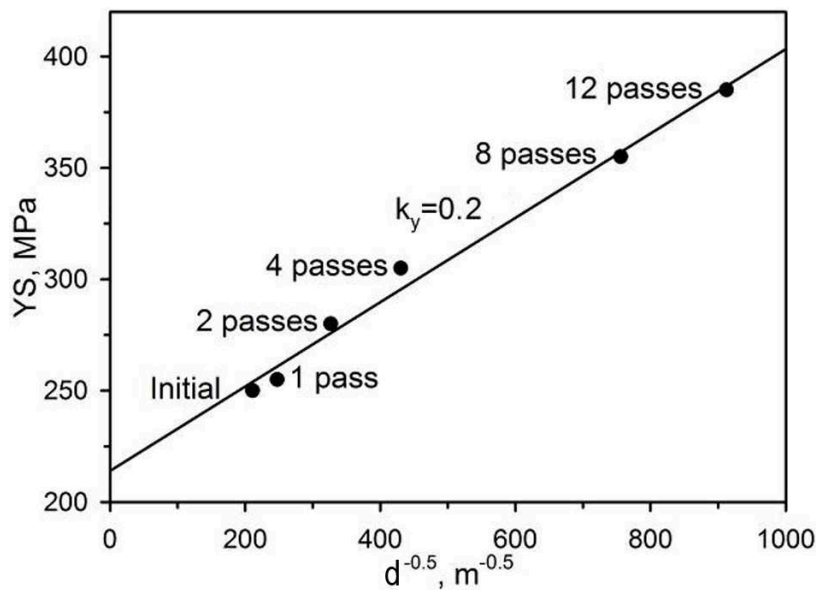


Fig.6. Relationship between the offset YS and the grain size

The YS values were plotted against $d^{-1/2}$ in Fig.6 to check the validity of the Hall-Petch relationship (1). The average grain size, d , was calculated as an average distance between HABs. As it was shown above this approach for determination of grain size is oversimplified taking into account that there exist two different structure component, which are distinctly distinguished by size and shape of grains, at all strains examined. However, as a first approximation, this approach provides information for Hall-Petch response of the 1570Al in a wide range of grain sizes. Experimental datum points

were fitted to straight line with a high accuracy (Fig.6) despite a great difference in dislocation density and density of LABs between deformation structures produced by different number of passes. The σ_0 and k_y values were calculated as 230 MPa and 0.2 MPa \times m^{1/2}, respectively, that is in a good agreement with data of work [7] for the 1570Al belonging to the first generation of Al-Mg-Sc alloys and Al-Mg alloy containing no Sc or Zr additives [8,9]. It is obvious that the introducing of coherent Al₃(Sc,Zr) provides +90% increase in friction stress and has no effect on the Hall-Petch slop [8], which remains at sufficiently low level. Re-calculation of data [7] shows that extensive grain refinement down to 80 nm in the 1570Al has to provide the YS of 620 MPa, only. It seems that +47% difference between the YS calculated in the present work and experimental YS reported in work [7] is attributed to the operation of other strengthening mechanisms. Primarily, deformation hardening may provide such increment in the YS [7] if dislocation density will attain $\rho \sim 2 \times 10^{15}$ m⁻². However, authors [7] did not report the exact dislocation density.

Summary

The Hall – Petch relationship has been examined in an Al-6%Mg-0.5Mn-0.2Sc-0.07Zr alloy in a wide grain size range. It has been established that the friction stress is 230 MPa and the Hall-Petch slope is of 0.2 MPa \times m^{1/2}. Mechanical properties of this alloy subjected to intense plastic straining could be interpreted with validity taking into account only that grain size strengthening and deformation hardening give significant contribution to the overall strength, concurrently.

Acknowledgement

Financial support from The Ministry of Education and Science of Russian Federation (project 14.A18.21.1983) is gratefully acknowledged. The authors also would like to thank a staff of Joint Research Center at Belgorod State University for technical assistance.

References

- [1] I.J. Polmear IJ, *Light Alloys. From traditional alloys to nanocrystals.* fourth ed., Butterworth-Heinemann/Elsevier, UK, 2006.
- [2] Yu.A. Filatov, V.I. Yelagin, V.V. Zakharov, *New Al-Mg-Sc alloys*, *Mater.Sci.Eng.* A280 (2000) 97–101.
- [3] J. Røyset, N. Ryum, *Scandium in aluminium alloys*, *Intern.Mater.Rev.* 50 (2005) 19-44.
- [4] R. Kaibyshev, A. Mogucheva, A. Dubyna, *Strategy for achieving high strength in Al-Mg-Sc alloys by intense plastic straining*, *Mater. Sci. Forum* 55 (2012) 706-709.
- [5] K.-T. Park, J.H. Park, Y.S. Lee, W.J.Nam, *Microstructures developed by compressive deformation of coarse grained and ultrafine grained 5083 Al alloys at 77 K and 298 K*, *Mater.Sci.Eng.* A408 (2005) 102-109.
- [6] M.A. Munoz-Morris, C. G. Oca, D.G. Morris, *Mechanical behaviour of dilute Al-Mg alloy processed by equal channel angular pressing*, *Scr.Mater.* 48 (2003) 213-218.
- [7] R.Z. Valiev, N.A. Enikeev, M.Yu. Murashkin, V.U. Kazykhanov, X. Sauvage, *On the origin of extremely high strength of ultrafine-grained Al alloys produced by severe plastic deformation*, *Scr. Mater.* 63 (2010) 949–952.
- [8] D.J. Lloyd, S.A. Court, *Influence of grain size on tensile properties of Al-Mg alloys*, *Mater Sci Tech* 19 (2003) 1349-1354.
- [9] H. Hasegawa, S. Komura, A. Utsunomiya, Z. Horita, M. Furukawa, M. Nemoto, T.G. Langdon, *Thermal stability of ultrafine-grained aluminum in the presence of Mg and Zr additions*, *Mater Sci Eng.* A265 (1999) 188-196.
- [10] O. Sitdikov, T. Sakai, E. Avtokratova, R. Kaibyshev, K. Tsuzaki, Y. Watanabe, *Microstructure behavior of Al-Mg-Sc alloy processed by ECAP at elevated temperature*, *Acta Mater.* 56 (2008) 821-834.
- [11] A. Mogucheva, E. Babich, B. Ovsyannikov, R. Kaibyshev, *Microstructural evolution in a 5024 aluminum alloy processed by ECAP with and without back pressure*, *Mater.Sci.Eng.* A560 (2013) 178–192.
- [12] H.W. Zhang, X. Huang, R. Pippin, N. Hansen, *Thermal behavior of Ni (99.967% and 99.5% purity) deformed to an ultra-high strain by high pressure torsion*, *Acta Materialia* 58 (2010) 1698–1707.
- [13] H. Halim, D.S. Wilkinson, M. Niewczas, *The Portevin-Le Chatelier (PLC) effect and shear band formation in an AA5754 alloy*, *Acta Mater.* 55 (2007) 4151-4160.

THERMEC 2013 Supplement

10.4028/www.scientific.net/AMR.922

Hall-Petch Relationship in an Al-Mg-Sc Alloy Subjected to ECAP

10.4028/www.scientific.net/AMR.922.120

DOI References

- [2] Yu.A. Filatov, V.I. Yelagin, V.V. Zakharov, New Al-Mg-Sc alloys, *Mater. Sci. Eng. A280* (2000) 97-101.
[http://dx.doi.org/10.1016/S0921-5093\(99\)00673-5](http://dx.doi.org/10.1016/S0921-5093(99)00673-5)
- [3] J. Røyset, N. Ryum, Scandium in aluminium alloys, *Intern. Mater. Rev.* 50 (2005) 19-44.
<http://dx.doi.org/10.1179/174328005X14311>
- [5] K. -T. Park, J.H. Park, Y.S. Lee, W.J. Nam, Microstructures developed by compressive deformation of coarse grained and ultrafine grained 5083 Al alloys at 77 K and 298 K, *Mater. Sci. Eng. A408* (2005) 102-109.
<http://dx.doi.org/10.1016/j.msea.2005.07.040>
- [6] M.A. Munoz-Morris, C. G. Oca, D.G. Morris, Mechanical behaviour of dilute Al-Mg alloy processed by equal channel angular pressing, *Scr. Mater.* 48 (2003) 213-218.
[http://dx.doi.org/10.1016/S1359-6462\(02\)00501-8](http://dx.doi.org/10.1016/S1359-6462(02)00501-8)
- [7] R.Z. Valiev, N.A. Enikeev, M. Yu. Murashkin, V.U. Kazykhanov, X. Sauvage, On the origin of extremely high strength of ultrafine-grained Al alloys produced by severe plastic deformation, *Scr. Mater.* 63 (2010) 949-952.
<http://dx.doi.org/10.1016/j.scriptamat.2010.07.014>
- [8] D.J. Lloyd, S.A. Court, Influence of grain size on tensile properties of Al-Mg alloys, *Mater Sci Tech* 19 (2003) 1349-1354.
<http://dx.doi.org/10.1179/026708303225006088>
- [9] H. Hasegawa, S. Komura, A. Utsunomiya, Z. Horita, M. Furukawa, M. Nemoto, T.G. Langdon, Thermal stability of ultrafine-grained aluminum in the presence of Mg and Zr additions, *Mater Sci Eng. A265* (1999) 188-196.
[http://dx.doi.org/10.1016/S0921-5093\(98\)01136-8](http://dx.doi.org/10.1016/S0921-5093(98)01136-8)
- [10] O. Sitdikov, T. Sakai, E. Avtokratova, R. Kaibyshev, K. Tsuzaki, Y. Watanabe, Microstructure behavior of Al-Mg-Sc alloy processed by ECAP at elevated temperature, *Acta Mater.* 56 (2008) 821-834.
<http://dx.doi.org/10.1016/j.actamat.2007.10.029>
- [11] A. Mogucheva, E. Babich, B. Ovsyannikov, R. Kaibyshev, Microstructural evolution in a 5024 aluminum alloy processed by ECAP with and without back pressure, *Mater. Sci. Eng. A560* (2013) 178-192.
<http://dx.doi.org/10.1016/j.msea.2012.09.054>
- [12] H.W. Zhang, X. Huang, R. Pippan, N. Hansen, Thermal behavior of Ni (99.967% and 99.5% purity) deformed to an ultra-high strain by high pressure torsion, *Acta Materialia* 58 (2010) 1698-1707.
<http://dx.doi.org/10.1016/j.actamat.2009.11.012>
- [13] H. Halim, D.S. Wilkinson, M. Niewczas, The Portevin-Le Chatelier (PLC) effect and shear band formation in an AA5754 alloy, *Acta Mater.* 55 (2007) 4151-4160.
<http://dx.doi.org/10.1016/j.actamat.2007.03.007>